Hindawi
Journal of Nanomaterials
Volume 2023, Article ID 9845438, 1 page
https://doi.org/10.1155/2023/9845438

Retraction

Retracted: Infrared Spectroscopic Measurement of Dissolved Organic Matter and Nanomaterials in Water Based on Parallel Factor Algorithm

Journal of Nanomaterials

Received 1 August 2023; Accepted 1 August 2023; Published 2 August 2023

This article has been retracted by Hindawi following an investigation undertaken by the publisher [1]. This investigation has uncovered evidence of one or more of the following indicators of systematic manipulation of the publication process:

(1) Discrepancies in scope
(2) Discrepancies in the description of the research reported
(3) Discrepancies between the availability of data and the research described
(4) Inappropriate citations
(5) Incoherent, meaningless and/or irrelevant content included in the article
(6) Peer-review manipulation

The presence of these indicators undermines our confidence in the integrity of the article's content and we cannot, therefore, vouch for its reliability. Please note that this notice is intended solely to alert readers that the content of this article is unreliable. We have not investigated whether authors were aware of or involved in the systematic manipulation of the publication process.

Wiley and Hindawi regrets that the usual quality checks did not identify these issues before publication and have since put additional measures in place to safeguard research integrity.

We wish to credit our own Research Integrity and Research Publishing teams and anonymous and named external researchers and research integrity experts for contributing to this investigation.

The corresponding author, as the representative of all authors, has been given the opportunity to register their agreement or disagreement to this retraction. We have kept a record of any response received.

References

[1] L. Liang, "Infrared Spectroscopic Measurement of Dissolved Organic Matter and Nanomaterials in Water Based on Parallel Factor Algorithm," *Journal of Nanomaterials*, vol. 2022, Article ID 5917198, 7 pages, 2022.

Hindawi
Journal of Nanomaterials
Volume 2022, Article ID 5917198, 7 pages
https://doi.org/10.1155/2022/5917198

Research Article

Infrared Spectroscopic Measurement of Dissolved Organic Matter and Nanomaterials in Water Based on Parallel Factor Algorithm

Li Liang

Chongqing Industry Polytechnic College, Choongqing, 401120, China

Correspondence should be addressed to Li Liang; 19402382@masu.edu.cn

Received 7 July 2022; Revised 24 July 2022; Accepted 30 July 2022; Published 24 August 2022

Academic Editor: S.K. Khadheer Pasha

Infrared spectroscopy can separate carbon sugars and amino sugars that have collapsed in soil water very quickly. In this study, the midinfrared (MIR) and near-infrared (NIR) spectra collected from soil water isolates or soil masses are sentenceless, assessing different agricultural groupings of flooded carbon and aminosaccharides. Soil was collected from five fields in two regions in western Canada and two regions in eastern Canada, where least squares backslide (PLSr) was inadequate. The inverted model of DOC recovery at the Eastern Peace River estuary can provide the optical functionality of traditional systems. The introduction of overflow DOCs from various sources rather than distance meters has been found to be a major contributor to the complexity of optical neighborhoods, resulting in a bias in DOC evaluation. The impact of voluntary DOC liability on the relationship between DOC and CDOM can be forgotten at a critical turn in the CDW. A slightly mitigating approach can overlook the impact of voluntary DOC responsibility on the relationship between DOC and CDOM. CDW is responsible for the continued responsibility of the Subei coastal currents for the normal material of the former Yellow Sea Delta, for the warm West Coast currents of the Yellow Sea for the materials of the Yellow Sea, and for the materials of the Changjiang Basin. The results of this study more thoroughly assess the state differences of DOM inputs from different sources within the CDW to determine the magnitude of the impact on DOC evaluation across the East China Sea CDOM. It suggests that it is necessary.

1. Introduction

The Changjiang River, the third longest river in the world, releases 0.5-0.8% of the river's dissolved organic carbon (DOC) into seawater [1], the East China Sea (ECS) and the Western Pacific Ocean. Close monitoring of the progress of DOC to ECS and its temporary fluctuations determines whether the Yangtze River estuary is a carbon sink or carbon producer and their importance to the global carbon balance. Recently, in order to spread the DOC inversion algorithm in consideration of huge satellite remote sensing and continuous monitoring function and to accumulate DOC material using large-scale satellite remote sensing and continuous monitoring function, a great deal of effort has been made. However, no practicable solution that is all-encompassing and suited for the Changjiang Estuary has been established as shown in Figure 1.

Hydrological issues normally include immense measures of information, confounded or briefly obscure components, and nondirect spatial and worldly circulation. Fake brain organizations (ANNs) can be utilized to display and take care of issues while building hydrological models. While applying this strategy for information investigation, the model plan is simply connected with the info and result information, and there is compelling reason need to dive into the nitty gritty instrument engaged with the genuine interaction relating to the model. In 1970, in view of ANNs, a self-arranging map (SOM) strategy was created and mostly utilized for information bunching, gathering, assessment, expectation, and information mining.

2. Materials and Procedures

2.1. Sampling and the Hydrodynamic Environment. The ECS, which consists of a massive continental rack, is one of the greatest marginal oceans on the planet. The extensive influences of various wellsprings of earthly material and intricate

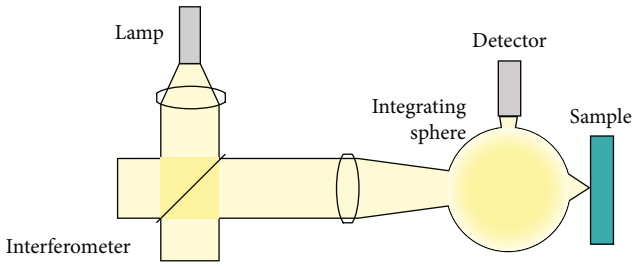

Figure 1: Infrared spectroscopic measurement.

hydrodynamic maritime cycles are responsible for the ECS's spatial and temporal transport of chemicals. The movement, dissemination, and the CDW's migration path and magnitude impact how materials mix in the ECS. Because of flood release, land causes, wind pressure, and different varieties experienced while confronting the saline Taiwan warm current, the CDW significantly turns regular. In the winter, it migrates southeastward, and in the summer, it is eccentric (TWC) as shown in Figure 2.

As the TWC enters the ECS's internal framework with a 50 m isobate near the entrance to the Yangtze River, the CDW will shift its development direction from southeast to east or perhaps east. The fan-like position between the PN sector and the F sector is affected by the muzzle combination. The fan-shaped region between regions PN and F is affected by estuary water (achieved by alternating new CDW and saltwater seawater) from either the Subei coastal current (SCC) or the Yellow Sea Warm Western Coastal Current (YSWCC) and the warm flow of the yellow sea from the north (YSWC) [2–4] or from the sea side of the estuary [5–9]. 123-123300 is a place close to 123-123300 E. The intermixing of these one-of-a-kind streams creates a complex hydrodynamic environment. Countless more modest natural particles agglomerate, structure bigger totals, and sink at a quicker rate around here, creating ocean snow [10], which hinders a large portion of preventing CDW items from passing via 123 E. The abundant supply of supplements in this area stimulates China's main fishing zone (the Zhou Shan fishing region) (122-130 E, 29-33 N) [1].

2.2. Methods. Recorded spectroscopy research: the CDOM maintenance spectrum was determined using a UV perceptual spectrophotometer (Shimadzu UV-2550) and a 10 cm quartz cuvette extending in 1 nm increments over the 200-800 nm range. High-purity Milli-Q water was used as a control.

$$a(\lambda) = 2.303 \times \frac{D(\lambda)}{L}, \quad (1)$$

where L is the length of the cuvette path, $a(\lambda)$ is the repeat assimilation factor, and $D(\lambda)$ is the optical depth of the repeat. Sg is the highest gradient of the CDOM maintenance spectrum that cannot be maintained indefinitely using equation (2) [11].

$$a(\lambda) = a(\lambda 0)e\mathrm{Sg}(\lambda 0 - \lambda) + k. \quad (2)$$

2.3. Analysis of Fluorescence Spectroscopy and PARAFAC. Fluorescence spectrophotometer Hitachi F-7000 was used to examine the CDOM's fluorescence spectrum (Hitachi High-Technologies, Tokyo, Japan). With a 5 nm range, the excitation recurrence was 200-450 nm. The repetition of the outpouring was 250-600 nm. The fluorescence spectra were obtained across a 1 nm range. To reduce the Raman dissipation of the pure water, the three-layered fluorescence scope of Milli-Q ultrapure water was deducted. The fluorescence arrangement was done with quinine sulphate (0.01 mg L1) [12].

2.3.1. DOC Measurements. Absolute organic carbon analyzer Shimadzu TOC-VCPH (temperature: 680°C, Shimadzu Co., Japan) was used to calculate the DOC focus. The DOC was changed over completely to CO2 using the high-temperature synergist oxidation (HTCO) approach; after that, a nondispersive infrared locator was utilized to measure it. Each incident was investigated twice, with a 2 percent standard deviation. The average worth was then used to calculate the DOC fixation. As a carbon standard, KHC8H4O4 was used. As a source of perspective, standard sea water with a referred to DOC was used. Every day, Milli-Q water spaces, both instrumental and procedural, were dismantled as shown in Table 1 and Figure 3 [13].

2.4. Chlorophyll-a, Suspended Sediments, and Salinity Measurements. Standard flour metric methods were used to calculate the fixation of chlorophyll-a (Chl-a). Turner Designs analyzed the fluorescence of each frozen Whitman GF/F channel. Fluor meter after separation with 90 percent (CH3)2CO (model 10) was used. This instrument was changed on a yearly basis using a Chl-a norm that was easily accessible (Sigma) [14].

3. Review of Literature

According to the ideal technique for determining water loss from soil and harvest overhang surfaces is to use extremely sensitive gauging or drifting lysimeters. It is a falsely enclosed volume of dirt that can be used to estimate input and surges of water, as well as check and gauge variations away. This method is utilized to properly estimate other water balance components like soil wetness capacity and deep seepage in a natural environment to calculate disappearing. In yield evapotranspiration research, the lysimeter is often utilized. It is used to examine genuine evapotranspiration results obtained using satellite data because of its precise estimation [15, 16].

3.1. Water Balance Approach. Apply the water balance condition to the catchment area of interest over time T and solve the evapotranspiration, ET, condition, as stated in the following equation:

$$\mathrm{ET} = P + Q + G + Q + G + S, \quad (3)$$

where P denotes precipitation, Qin denotes surface water inflow, Qout denotes surface water surge, Gin denotes ground water intake, Gout denotes ground water outpouring, and S is

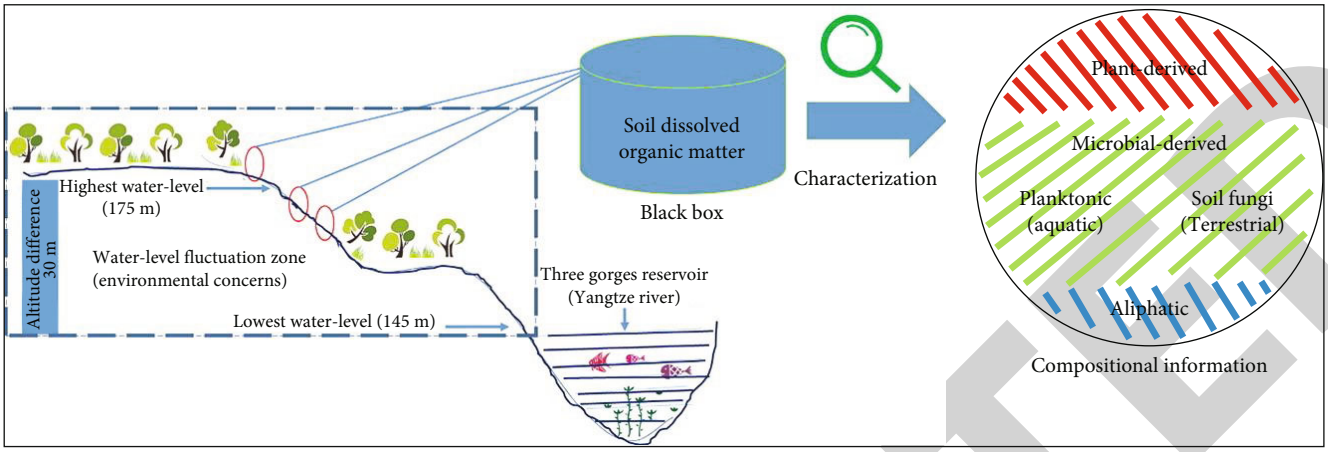

Figure 2: Taiwan warm current.

Table 1: DOC measurements.

Scale	Mean	Range	SD	CV (%)
Western	1022	4605	4606	4607
Eastern	1023	1024	1025	1026
Multisite	4402	1025	1026	1027
Western	1022	4605	4606	4607
Western	1022	4605	4606	4607
Eastern	1023	1024	1025	1026
Multisite	4402	1025	1026	1027

the shift in how much water is put away with time, assuming long-term irrelevant change away.

According to in a new report done at a substicky area in India, it was found that FAO-56 Penman-Monteith gauges contrasted most well and ETpot values estimated in a grass lysimeter and yielded normal root mean square blunder (RMSE) of 0.08 mm/day. Exhibitions of a few generally utilized ETpot techniques were assessed comparatively with the FAO-56 suggested Penman-Monteith strategy for a scope of climatic circumstances predominant in India. It additionally expresses that temperature-related factors seem, by all accounts, to be the most urgent information sources expected to acquire ETpot gauges.

According to for the most part, evapotranspiration is calculated utilizing satellite-derived TIR data and ground-based meteorological data as inputs to a single layered limit layer model. Pioneer works on utilizing TIR observations for estimating consumptive use in agriculture [17].

According to evapotranspiration assessment from remote detecting-based energy balance models converts satellite detected radiances into land surface qualities, for example, surface albedo, leaf region record, vegetation files, surface emissivity, and surface temperature. While considering immediate circumstances, the following are the conditions for measuring ET as part of the land surface energy balance:

$$R : H + E : G. \tag{4}$$

3.2. Classification of Remote Sensing-Based Methods. According to ET is a geographical and transitory component since hydrological processes are dependent on weather and the environment. The interplay of the spatial and ephemeral elements of evapotranspiration processes results in a complex ET assessment system.

According to Courault et al. (2005), remote sensing-based methods of estimating ET are classified under four categories which are based on the following: techniques were directly worked on, residual methods for the energy budget, strategies that are deterministic, and a strategy based on the vegetation.

(Bastiaanssen et al. 1998a) SEBAL (Surface Energy Balance Algorithm for Land) is a methodology that uses both precise linkages and actual definitions. This model was created with the goal of determining energy partitioning at the territorial scale using the least amount of ground data possible. Anyway a large portion of the hypothesis and a significant part of the methods are satellite independent, and hence, the strategy can be utilized with other satellite pictures having warm groups. This model is used to analyze ET in various agricultural climatic conditions such as Spain, Turkey, Egypt, India, Sri Lanka, China, and the United States [18].

According to the Index of Simplified Surface Energy Balance (S-SEBI) is an upgraded edition of the SEBI that was built, tested, and authorised to identify information. They utilized Landsat TM information and observed that the deliberate and assessed evaporative portion values have a most extreme relative distinction of 8%. Fostered a Surface Energy Balance System (SEBS) based on the SEBI concept, which allows for the assurance of the Evaporative Fraction (EF) by processing the energy balance under constrained situations. This technique gauges motions from satellite information and regularly accessible meteorological information.

Water utilization of huge water system frameworks has been tended to with NOAA-AVHRR in Pakistan SEBAL was utilized to assess genuine evapotranspiration on a yearly scale across a tremendous waterway bowl framework with at least ground information. Just daylight term and wind speed are expected as information for the remote detecting transition calculation. They detailed that exactness of surveying the time

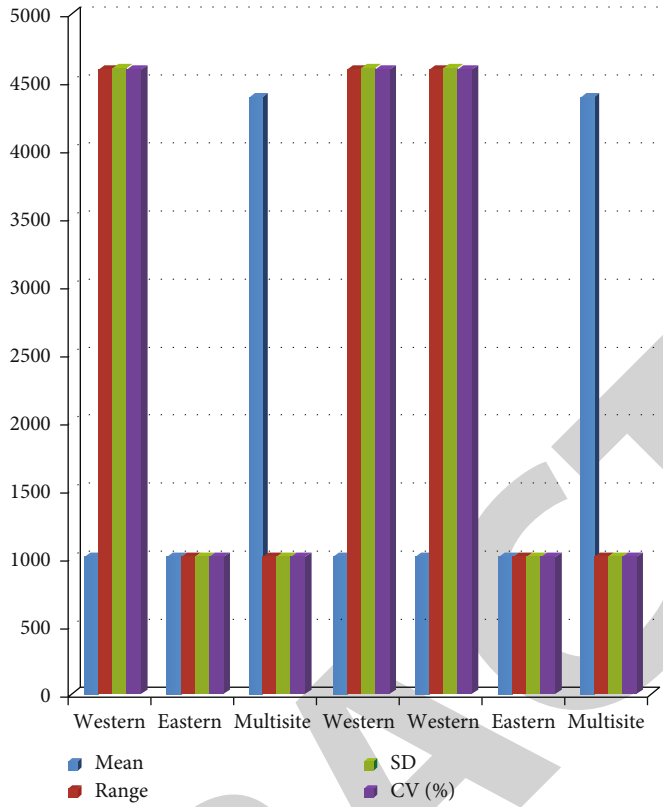

Figure 3: Mean and standard deviation value.

coordinated genuine yearly evapotranspiration fluctuated from 0 percentage to 10 percentage on a field scale to 5 percentage at the provincial level [2, 19–21].

4. DOC Source Analysis

Contribute to more DOCs and key DOC components along three separate sections to better understand how inconsistent DOC components affect the connection between CDOM and DOC. We have considered multiple DOC material sources that can shift. Due to the predominance of the erogenous zone, segment XM has the highest DOC occupancy, a (355), Fs (355), and C1 values and the lowest Sg value [53,80]. Nevertheless, very high values of DOC, a (355), Fs (355), C2, and C3 at stations XM04 and XM05 indicate wastewater infiltration from the Huangpu River as shown in Figures 4 and 5 [22, 23].

At station F07, a startlingly large amount of C2 was observed. Given its surprisingly high DOC center, this is predictable. Station F07 is located in a complicated stream environment where materials are exchanged and mixed abundant improvements sustain microscopic fish sprouts, and regular activities and organic trash decomposition form protein-like fluorescence tops [23]. Also, in the south of Jeju Island (125300 E-127 E), there is an upwelling structure with rich improvements, and the normal suspension of base development has been seen [24]. The presence of gathering interstitial water or possibly buildup suspension in the base water could bring about an increase in the force of protein-like C2 and DOC in surface ocean water during upwelling as a result of the base water's more grounded fluorescence power of tryptophan and tyrosine [23]. Nonetheless, at this station, a noteworthy drop in the a (355) regard was seen, implying that using a (355) to control marine CDOM has impediments and that regular DOC makes a restricted difference [24].

5. Atmospheric Correction

Although environmental influences can lead to erroneous results when extracting surface temperatures from TIR remote sensing data when left unchecked, they can be adjusted using PC modeling. Boundary evaluation and surface reflectance recovery are two key stages in the air repair process. Calculating climatic transmission and upwelling brilliance has always been a difficult and time-consuming process. A web-based tool for atmospheric correction was used.

6. Data Fusion

Right now, satellite sensors are created to give high ghastly, high spatial, and high worldly goal. A few late endeavors have endeavored to scaling issues are addressed by dismantling ET estimates based on autonomous multiresolution satellite sensors [25–28]. Yet, taking everything into account, getting the picture of high spatial goal and high phantom goal simultaneously is troublesome. The framework tradeoff

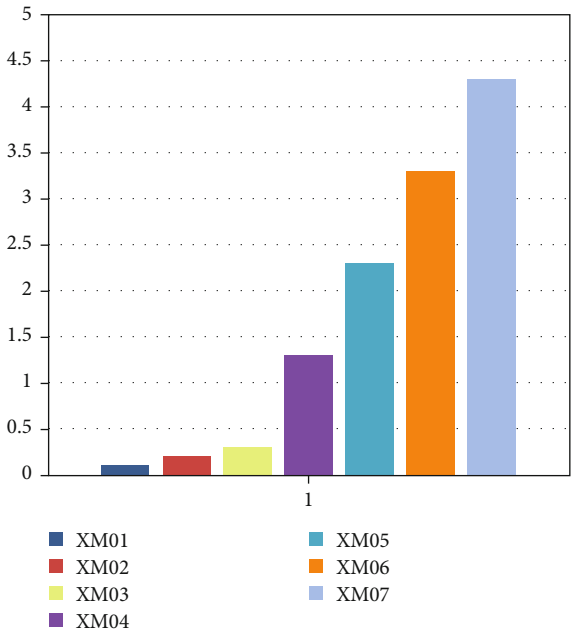

Figure 4: Between the CDOM and the DOC.

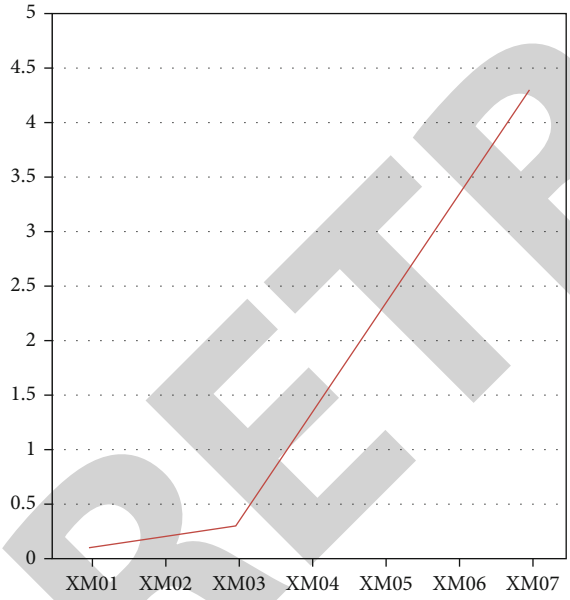

Figure 5: Observed at stations XM04 and XM05.

among spatial and other worldly goal remote detecting pictures tend to have either high spatial goal and low ghostly goal or the other way around. The data content of the single picture is restricted by the spatial and ghostly goal of the imaging framework. Both phantom data and spatial data of somewhat detected pictures are vital for remote detecting applications. The spatial upgrade of low spatial goal information acquired from something similar or different sensor is conceivable. One potential arrangement comes from the field of information combination.

$$R^2 = \frac{\sum_{i=1}^{n} y\left(y^2 - y^2\right)}{\sum_{i=1}^{n} y\left(y^2 - y^2\right)^2},$$

$$\text{RMSEC(RMSEP)} = \sqrt{\frac{1}{2}\sum_{I=1}^{N}(Y - Y)}, \tag{5}$$

$$\text{RPD}c(\text{RPD}p) = \frac{\text{SD}}{\text{RMSEC (or RMSEP)}}.$$

6.1. High Pass Filtering. The High Pass Filtering (HPF) combination approach is a specific application of number juggling procedures for intertwining symbology, involving math operations such as expansion, deduction, increase, and rationing. Before combining the two informative indexes on a pixel-by-pixel basis, HPF applies a spatial upgrading channel to the high-resolution image. Using a band expansion method, the HPF combination integrates both spatial and ghostly information. When compared to IHS and PCA, discovered that the HPF technique exhibits less contortion in the ghostly properties of the information, and bends were small and difficult to detect. This goal required a quantitative, visual, and graphical analysis of the information's heinous features. The main drawback of the HPF technique is that the results are very much dependent on the window size over which the high frequency detail image is computed. This technique laid the foundation for advanced multiresolution analysis (MRA) [13, 29].

7. Multiresolution Analysis-Based Methods

The MRA-based methods use the same principle as the HPF technique. They extract the high frequency or detail information from the high-resolution image for insertion into the low-resolution image. The difference lies in the way in which this information is extracted [30, 31]. The MRA transforms perform. A forward filter is used to separate the information with low and high frequency in the photograph transformation is used to substitute the high frequency information from the high spatial resolution into the low spatial resolution image and finally perform a reverse transform to construct the spatially.

The center standard of the MRA-based techniques is the partition of the low and high frequencies in the pictures and subbing the high recurrence data of the great goal picture into the low goal pictures [32–34]. The different MRA changes that have been utilized in spatial goal improving examination are as follows:

(i) Discrete wavelet transform (DWT)

(ii) Excess wavelet transform (RWT)

(iii) A trous wavelet transform (AWT)

(iv) Laplacian pyramid (LP)

7.1. Spatial Resolution Enhancement. To spatially enhance the collected images, techniques take advantage of the complimentary spatial/spectral resolution properties of imaging

sensors. Fusion of data based on MRA requires a model to describe about how 46 the spatial details of high-resolution image are to be injected into the coarse resolution image. Discuss the concept of injecting high frequencies in the low-resolution images. Several strategies for integrating high- and low-resolution data to improve the spatial resolution of low-resolution images have been proposed. Some of the more commonly utilized ones were described in the previous section [12].

8. Conclusions

The complete dataset includes the southern part of the Yangtze River (XM region), the main center, and the northern limits of CDWs such as sections PN and F. In this review, we investigated the relationship between the optical properties of CDOM and doctor. These sections described the absorption and fluorescence properties of CDOM, as well as the potential causes of increased DOC uptake. We investigated the ability of the CDOM's optics to reflect key intrinsics that affect the relationship between the DOC's optics and the CDW's CDOM, regardless of the hydrodynamic climate, phytoplankton, and microbiological activities, as well as DOC variations and their associations. The accompanying endings, in particular, were drawn in light of the implications of this review. DOC, in general, behaves moderately, and the weakening of earthbound CDW-moved material has the upper hand in determining DOC dissemination characteristics and CDOM optical qualities [14, 35]. In the three segments, The contaminated water from the Huang pujiang River, in particular, will supply DOC that has been miscalculated, on the off chance that information is utilized without wary screening. From the Yellow Sea shipped by the SCC, terrestrial material from the Yellow Sea basin, primarily from the former Yellow Sea Delta, and earth-bound material from the Yangtze River basin, provided by the CDW, were transported from the Yellow Sea provided by the YSWCC. Piece F can be one of the main reasons for DOC and CDOM optical quality errors. In any case, the monstrosity of Huanghe River Bowl's steady material responsibility merits more thought. The DOC and CDOM effects of autochthonous DOC commitment of the association amount in the PN region can be ignored in conjunction with the modest weakening method on the important center point of CDW [21].

Data Availability

The data used to support the findings of this study are included within the article.

Conflicts of Interest

The authors declare that they have no conflicts of interest.

Acknowledgments

The Chongqing Natural Science Foundation provided funding for this research (No. cstc2021jcyj-msxmX1065).

References

[1] Q. Y. Sun, C. Wang, P. F. Wang, J. Hou, and Y. H. Ao, "Absorption and fluorescence characteristics of chromophoric dissolved organic matter in the Yangtze Estuary," *Environmental Science and Pollution Research*, vol. 21, no. 5, pp. 3460–3473, 2014.

[2] X. Sun, *Chinese Offshore Marine Area (Chinese Edition)*, Ocean Press, Beijing, China, 2006.

[3] D. X. Hu, "Some striking features of circulation in Huanghai Sea and East China Sea," in *Oceanology of China Seas*, pp. 27–38, Springer, Dordrecht, The Netherlands, 1994.

[4] L. Qi, C. Hu, H. Duan, B. Barnes, and R. Ma, "An EOF-based algorithm to estimate chlorophyll a concentrations in Taihu Lake from MODIS land-band measurements: implications for near real-time applications and forecasting models," *Remote Sensing*, vol. 6, no. 11, pp. 10694–10715, 2014.

[5] L. J. Zhang, J. Y. Zang, M. A. Y. Xing et al., "Variability and influence of dissolved silica in the Qiangtangjiang Estuary," *Marine Sciences*, vol. 8, pp. 51–57, 2015.

[6] L. K. Kang, H. M. Lu, P. T. Sung et al., "The summer distribution of coccolithophores and its relationship to water masses in the East China Sea," *Journal of Oceanography*, vol. 72, no. 6, pp. 883–893, 2016.

[7] B. Han, X. Zhang, J. Yang, and J. Pei, "Multiple-height analytical continuation in processing the gravity anomaly data from the East China Sea and adjacent regions," *Chinese High Technology Letters*, vol. 17, pp. 1272–1277, 2007.

[8] H. Ogawa and E. Tanoue, "Dissolved Organic Matter in Oceanic Waters," *Journal of Oceanography*, vol. 59, pp. 129–147, 2003.

[9] M. Aoyama and K. Hirose, "Radiometric determination of anthropogenic radionuclides in seawater," *Radioactivity in the Environment*, vol. 11, pp. 137–162, 2008.

[10] B. Deng, J. Zhang, and Y. Wu, "Recent sediment accumulation and carbon burial in the East China Sea," *Global Biogeochemical Cycles*, vol. 20, pp. 1–12, 2006.

[11] Y. Li, G. Song, S. Hu, and H. Xie, "Optical characterization, distribution and sources of chromophoric dissolved organic material (CDOM) in the Changjiang river estuary in July 2014," *Oceanologia et Limnologia Sinica/Hai Yang Yu Hu Chao*, vol. 46, pp. 670–678, 2015.

[12] Q. Zhou, R. Su, Y. Bai, C. Zhang, and X. Shi, "Characterization of chromophoric dissolved organic matter (CDOM) in Zhoushan fishery using excitation-emission matrix spectroscopy (EEMs) and parallel factor analysis (PARAFAC)," *Environmental Sciences*, vol. 36, pp. 163–171, 2015.

[13] Q. Liu, D. Pan, Y. Bai et al., "The satellite reversion of dissolved organic carbon (DOC) based on the analysis of the mixing behavior of DOC and colored dissolved organic matter: the East China Sea as an example," *Acta Oceanologica Sinica*, vol. 32, pp. 1–11, 2013.

[14] X. L. Yu, F. Shen, and Y. Y. Liu, "Light absorption properties of CDOM in the Changjiang (Yangtze) estuarine and coastal waters: an alternative approach for DOC estimation," *Estuarine, Coastal and Shelf Science*, vol. 181, pp. 302–311, 2016.

[15] L. Bodineau, G. Thournelin, V. Beghin, and M. Wartel, "Tidal time-scale changes in the composition of particulate organic matter within the estuarine turbidity maximum zone in the macrotidal Seine Estuary, France: the use of fatty acid and sterol biomarkers," *Estuarine, Coastal and Shelf Science*, vol. 47, no. 1, pp. 37–49, 1998.

[16] M. B. Alazzam, W. T. Mohammad, M. B. Younis et al., "Studying the effects of cold plasma phosphorus using physiological and digital image processing techniques," *Computational and Mathematical Methods in Medicine*, vol. 2022, 5 pages, 2022.

[17] L. Y. Yang, W. Chen, W. E. Zhuang et al., "Characterization and bioavailability of rainwater dissolved organic matter at the southeast coast of China using absorption spectroscopy and fluorescence EEM-PARAFAC," *Estuarine, Coastal and Shelf Science*, vol. 217, pp. 45–55, 2019.

[18] L. M. William and A. M. Mary, "Interaction of photochemical and microbial processes in the degradation of refractory dissolved organic matter from a coastal marine environment," *Limnology and Oceanography*, vol. 42, pp. 1317–1324, 1997.

[19] N. B. Nelson, D. A. Siegel, and A. F. Michaels, "Seasonal dynamics of colored dissolved material in the Sargasso Sea," *Deep Sea Research Part I: Oceanographic Research Papers*, vol. 45, no. 6, pp. 931–957, 1998.

[20] C. Lin, X. Ning, J. Su, Y. Lin, and B. Xu, "Environmental changes and the responses of the ecosystems of the Yellow Sea during 1976–2000," *Journal of Marine Systems*, vol. 55, pp. 223–234, 2004.

[21] Q. S. Wei, Z. G. Yu, B. D. Wang et al., "Coupling of the spatial-temporal distributions of nutrients and physical conditions in the southern Yellow Sea," *Journal of Marine Systems*, vol. 156, pp. 30–45, 2016.

[22] L. S. Alan and D. T. Jonathan, "Marine snow: microscale nutrient patched," *Limnology and Oceanography*, vol. 24, pp. 850–854, 1979.

[23] A. Abdullah Hamad, M. Lellis Thivagar, M. Bader Alazzam et al., "Dynamic systems enhanced by electronic circuits on 7D," *Advances in Materials Science and Engineering*, vol. 2021, Article ID 8148772, 11 pages, 2021.

[24] M. Fu, Z. Wang, Y. Li et al., "Phytoplankton biomass size structure and its regulation in the Southern Yellow Sea (China): seasonal variability," *Continental Shelf Research*, vol. 29, no. 18, pp. 2178–2194, 2009.

[25] S. Y. Wang and J. P. Liu, "Delving into the relationship between autumn Arctic sea ice and central–eastern Eurasian winter climate," *Atmospheric and Oceanic Science Letters*, vol. 9, pp. 366–374, 2016.

[26] C. C. Chen, G. C. Gong, and F. K. Shiah, "Hypoxia in the East China Sea: one of the largest coastal low-oxygen areas in the world," *Marine Environmental Research*, vol. 64, no. 4, pp. 399–408, 2007.

[27] B. Wang, J. Hu, S. Li, and D. Liu, "Anumerical analysis of biogeochemical controls with physical modulation on hypoxia during summer in the Pearl River estuary," *Biogeosciences*, vol. 14, pp. 1–31, 2017.

[28] R. M. Cory and D. M. McKnight, "Fluorescence spectroscopy reveals ubiquitous presence of oxidized and reduced quinones in dissolved organic matter," *Environmental Science & Technology*, vol. 39, no. 21, pp. 8142–8149, 2005.

[29] Y. S. Younis, A. H. Ali, O. K. Alhafidhb et al., "Early diagnosis of breast cancer using image processing techniques," *Journal of Nanomaterials*, vol. 2022, Article ID 2641239, 6 pages, 2022.

[30] G. C. Cui, L. Zhu, L. H. Gui, Q. B. Zhao, J. H. Zhang, and J. T. Cao, "Multidimensional clinical data denoising via Bayesian CP factorization," *Science China-Technological Sciences*, vol. 63, no. 2, pp. 249–254, 2020.

[31] C. W. Cuss and C. Gueguen, "Analysis of dissolved organic matter fluorescence using self-organizing maps: mini-review and tutorial," *Analytical Methods*, vol. 8, no. 4, pp. 716–725, 2016.

[32] L. Li, Y. Wang, W. Zhang, S. Yu, X. Wang, and N. Gao, "New advances in fluorescence excitation-emission matrix spectroscopy for the characterization of dissolved organic matter in drinking water treatment: a review," *Chemical Engineering Journal*, vol. 381, article 122676, 2020.

[33] W. Chen and H. Q. Yu, "Advances in the characterization and monitoring of natural organic matter using spectroscopic approaches," *Water Research*, vol. 190, article 116759, 2021.

[34] R. Yang, Z. Li, M. Huang, N. Luo, J. Wen, and G. Zeng, "Characteristics of fulvic acid during coprecipitation and adsorption to iron oxides-copper aqueous system," *Journal of Molecular Liquids*, vol. 274, pp. 664–672, 2019.

[35] X. Y. Zhang, X. Chen, H. Deng, Y. Du, and H. Y. Jin, "Absorption features of chromophoric dissolved organic matter (CDOM) and tracing implication for dissolved organic carbon (DOC) in Changjiang Estuary, China," *Biogeosciences Discussions*, vol. 101, pp. 2217–12250, 2013.